The diffusion equation: Analytical and numerical solutions in one and two spatial dimensions applied to studying the temperature distribution of the lithosphere

James Claxton, Amund Fredriksen

December 18, 2020

Abstract

The diffusion equation was solved analytically and numerically. The explicit scheme, the implicit scheme and the Crank-Nicolson scheme for numerically solving the one dimensional diffusion equation were implemented and tested. The algorithms based on the implicit and Crank-Nicolson schemes both outperformed the explicit scheme algorithm, and they were seen to have a similar level of accuracy. Jacobi's iterative method was implemented and tested to solve the two dimensional diffusion equation in the implicit scheme. Using these algorithms and tests it was found that at present the mantle on the west coast of Norway is at maximum $292\,\mathrm{K}$ hotter than normal mantle if it had been enriched with Uranium, Thorium and Potassium $1\,\mathrm{Gyr}$ ago.

1 Introduction

How things spread or diffuse is an ubiquitous phenomenon in nature. A simple example is when a drop of dye is dropped into a water container and the dye spreads out in the water. Another example is from fluid dynamics when there is water between two parallel plates moving with different velocities, in which case the velocity of the water flow will diffuse from the faster plate towards the slower plate. Yet another example, which is the case we will study in this report, is when there is a temperature gradient between two points and heat diffuses through the material or medium from the hotter point to the colder point.

Diffusion processes can be described mathematically by the diffusion equation. Solving this equation enables us to see quantitatively how some quantity, e.g. temperature, diffuses through space in time. In this report we present numerical simulations, retrieved from solving the diffusion equation, of how temperature distributions evolve in time given specified boundary- and initial conditions of the system. These solutions are calculated both for the case of one spatial dimension and for two spatial dimensions. Analytical solutions are also presented, and the numerical methods are compared to the analytical solutions in order to check their accuracies.

In the final part of the report the temperature distribution in the lithosphere on the western coast of Norway is studied. It is proposed that on the west coast there was an active subducting zone about $1\,\mathrm{Gyr}$ ago [1, 2]. Due to this subducting zone the mantle is re-fertilised with radioactive elements and is expected to more enriched with these elements than normal mantle [3]. The temperature evolution of this mantle is studied in this report to simulate the changes in temperature expected due to these radioactive elements.

2 Theory

2.1 The diffusion equation

The diffusion equation is a partial differential equation which has the form

$$\nabla^2 u(\mathbf{x}, t) = D \frac{\partial u(\mathbf{x}, t)}{\partial t}, \tag{2.1}$$

where D is a constant called the diffusion coefficient or diffusivity and $\nabla^2 \equiv \frac{\partial^2}{\partial x^2} + \frac{\partial^2}{\partial y^2} + \frac{\partial^2}{\partial z^2}$. D has dimensions time/length^2. This equation is quite general, and $u(\mathbf{x}, t)$ is not restricted to one specific physical meaning. u represents the quantity that is diffused, examples of which were mentioned in the introduction, for example the temperature at some point in space and time, or it can represent the velocity of the fluid flow between two infinite parallel plates with a relative velocity. A solution $u(\mathbf{r}, t)$ to the diffusion equation gives how u spreads out in time from its initial state at $t = 0$, at any given point $\mathbf{x}$ in space. The conditions at the boundaries of the system also contribute to the time development of $u(\mathbf{r}, t)$.

We can get the diffusion equation to a simpler and dimensionless form. We can define new, dimensionless spatial variables $\hat{\mathbf{x}} \equiv (\hat{x}, \hat{y}, \hat{z})$ through $\alpha\hat{x} \equiv x$, $\alpha\hat{y} \equiv y$ and $\alpha\hat{z} \equiv z$ where α is some constant with dimension length, so $\alpha\hat{\mathbf{x}} \equiv \mathbf{x}$. Then the diffusion equation becomes

$$\frac{\partial^2 u}{\partial(\alpha\hat{x})^2} + \frac{\partial^2 u}{\partial(\alpha\hat{y})^2} + \frac{\partial^2 u}{\partial(\alpha\hat{z})^2} = \frac{1}{\alpha^2}\left(\frac{\partial^2 u}{\partial\hat{x}^2} + \frac{\partial^2 u}{\partial\hat{y}^2} + \frac{\partial^2 u}{\partial\hat{z}^2}\right) = D\frac{\partial u}{\partial t} \tag{2.2}$$

$$\Updownarrow \tag{2.3}$$

$$\frac{\partial^2 u}{\partial\hat{x}^2} + \frac{\partial^2 u}{\partial\hat{y}^2} + \frac{\partial^2 u}{\partial\hat{z}^2} \equiv \hat{\nabla}^2 u = \alpha^2 D \frac{\partial u}{\partial t} \equiv \frac{\partial u}{\partial \hat{t}}, \tag{2.4}$$

where $[\alpha^2 D] = \text{length}^2 \cdot (\text{time} \cdot \text{length}^{-2}) = \text{time}$ and we have defined the dimensionless variable $\hat{t} \equiv t/(\alpha D)$ and the dimensionless nabla operator $\hat{\nabla}^2 \equiv \frac{\partial^2}{\partial\hat{x}^2} + \frac{\partial^2}{\partial\hat{y}^2} + \frac{\partial^2}{\partial\hat{z}^2}$. So our dimensionless and simplified diffusion equation is

$$\hat{\nabla}^2 u(\hat{\mathbf{x}}, \hat{t}) = \frac{\partial u(\hat{\mathbf{x}}, \hat{t})}{\partial \hat{t}}. \tag{2.5}$$

In the subsequent parts of this report we will only use the dimensionless form of the diffusion equation, so for simplicity we will use the symbols x, y, z, t for the dimensionless variables instead of $\hat{x}, \hat{y}, \hat{z}, \hat{t}$.

2.2 Analytical solution to the diffusion equation in one dimension

The one-dimensional diffusion equation is the diffusion equation with only one spatial variable, so $\mathbf{x} \to x$. Then Eq. (2.5) becomes

$$\frac{\partial^2 u(x, t)}{\partial x^2} = \frac{\partial u(x, t)}{\partial t}. \tag{2.6}$$

For boundary conditions

$$u(0, t) = 0, \quad t \geq 0, \tag{2.7}$$

and

$$u(L, t) = 1, \quad t \geq 0, \tag{2.8}$$

and initial condition

$$u(x, 0) = 0, \quad 0 < x < L, \tag{2.9}$$

3

the final result for the solution of $u(x, t)$ is

$$u(x, t) = \frac{2}{\pi} \sum_{n=1}^{\infty} (-1)^n \frac{\sin(n\pi x/L)}{n} e^{-n^2\pi^2 t/L^2} + \frac{x}{L}. \tag{2.10}$$

The derivation of this solution can be found in appendix A.

2.3 Analytical solution to the diffusion equation in two dimensions

With two spatial dimensions the diffusion equation becomes

$$\frac{\partial^2 u(x, y, t)}{\partial x^2} + \frac{\partial^2 u(x, y, t)}{\partial y^2} = \frac{\partial u(x, y, t)}{\partial t}, \tag{2.11}$$

or

$$u_{xx} + u_{yy} = u_t. \tag{2.12}$$

In the two-dimensional case we can choose for simplicity our system to be a rectangular or square area. Boundary conditions must be specified on all points on the line defining the border of the system, in this case the four sides, and the initial condition must be defined on all points in the area enclosed by the boundaries. The boundary conditions we have chosen is $u(x, y, t) = 0$ along all the walls, that is, for $x = 0, L$ and for $y = 0, L$. The initial condition is chosen to be

$$u(x, y, t = 0) = \sin\left(\frac{\pi x}{L}\right) \sin\left(\frac{\pi y}{L}\right). \tag{2.13}$$

For these boundary- and initial conditions, the solution of the two-dimensional diffusion equation is

$$u(x, y, t) = \sin\left(\frac{\pi x}{L}\right) \sin\left(\frac{\pi y}{L}\right) e^{-2\pi^2 t/L^2}. \tag{2.14}$$

The derivation of this solution can be found in appendix B.

2.4 The algorithms for solving the diffusion equation in one dimension

Three slightly different algorithms are implemented for solving the heat equation. These methods are the forward Euler method, the backward Euler method and the Crank-Nicolson method.

2.4.1 The forward Euler method

The dimensionless diffusion equation is given by

$$\frac{\partial^2 u(x, t)}{\partial x^2} = \frac{\partial u(x, t)}{\partial t}, \tag{2.15}$$

or

$$u_{xx} = u_t, \tag{2.16}$$

where the solution u has both spacial and temporal dependencies x and t, respectively. We can discretise space with centred difference and discretise time with the forward Euler method. The right hand side of Eq. 2.16 goes to

$$u_t \approx \frac{u(x, t + \Delta t) - u(x, t)}{\Delta t} = \frac{u(x_i, t_j + \Delta t) - u(x_i, t_j)}{\Delta t}, \tag{2.17}$$

where Δt is the time step size, i and j are the spacial and time indices, respectively. The local approximation error goes like $O(\Delta t)$. The left hand side of Eq. 2.16 goes to

$$u_{xx} \approx \frac{u(x + \Delta x, t) - 2u(x, t) + u(x - \Delta x, t)}{\Delta x^2}, \tag{2.18}$$

or

$$u_{xx} \approx \frac{u(x_i + \Delta x, t_j) - 2u(x_i, t_j) + u(x_i - \Delta x, t_j)}{\Delta x^2}, \tag{2.19}$$

where Δx is the step size in the spacial dimension. The local approximation error goes like $O(\Delta x^2)$.

In a more simplified way where $u(x_i, t_j)$ is shortened to u_{ij} this can be written as

$$\frac{u_{i,j+1} - u_{i,j}}{\Delta t} = \frac{u_{i+1,j} - 2u_{i,j} + u_{i-1,j}}{\Delta x^2}, \tag{2.20}$$

or

$$u_{i,j+1} = \alpha u_{i+1,j} + (1 - 2\alpha)u_{i,j} + \alpha u_{i+1,j}, \tag{2.21}$$

where $\alpha = \Delta t / \Delta x^2$. It is written in this form, since $u_{i,j+1}$ is the only unknown in this equation. This results in a matrix vector multiplication given by

$$V_{j+1} = \hat{A}V_j = \hat{A}^2 V_{j-1} = ... = A^{\hat{j}+1}V_0, \tag{2.22}$$

where $\hat{A}$ is

$$\begin{vmatrix} 1\text{-}2\alpha & \alpha & 0 & ... & 0 \\ \alpha & 1\text{-}2\alpha & \alpha & ... & 0 \\ 0 & \alpha & ... & ... & ... \\ ... & ... & ... & ... & \alpha \\ 0 & 0 & ... & \alpha & 1\text{-}2\alpha \end{vmatrix}$$

The stability of the explicit scheme is limited however since it requires that $\Delta t / \Delta x^2 \leq 1/2$ [4].

2.4.2 The backward Euler method

We can also use the backward method in the same way to find the numerical solution to the diffusion equation. The right hand side of Eq. 2.16 is given by

$$u_t \approx \frac{u_{i,j} - u_{i,j-1}}{\Delta t} \tag{2.23}$$

which again has a local approximation error which goes like $O(\Delta t)$. The spacial derivative is given by

$$u_{xx} = \frac{u_{i+1,j} - 2u_{i,j} + u_{i-1,j}}{\Delta x^2}, \tag{2.24}$$

which has a local approximation error which goes like $O(\Delta x^2)$. By equating these two equations and putting $u_{i,j-1}$ to the left hand side gives

$$u_{i,j-1} = -\alpha u_{i-1,j} + (1 + 2\alpha)u_{i,j} - \alpha u_{i+1,j}. \tag{2.25}$$

This can be written as a matrix vector multiplication given by

$$V_j = \hat{A}^{-1}V_{j-1} = \hat{A}^{-1}(\hat{A}^{-1}V_{j-2}) = \hat{A}^{-j}V_0, \tag{2.26}$$

where $\hat{A}$ is

$$\begin{vmatrix} 1\text{+}2\alpha & \text{-}\alpha & 0 & ... & 0 \\ \text{-}\alpha & 1\text{+}2\alpha & \text{-}\alpha & ... & 0 \\ 0 & \text{-}\alpha & ... & ... & ... \\ ... & ... & ... & ... & \text{-}\alpha \\ 0 & 0 & ... & \text{-}\alpha & 1\text{+}2\alpha \end{vmatrix}$$

Unlike the explicit scheme, this method does not have any stability critieria and is valid for all Δt and Δx. This can be proven since the specral radius of $\hat{A}$ is less than one, i.e $\rho(\hat{A}) < 1$ [4]. Numerically Eq. 2.26 can be solved using the Thomas algorithm for a tri-diagonal matrix, which is much faster than for example using Gaussian elimination.

2.4.3 The Crank-Nicolson method

The Crank-Nicolson method is a combination of the two schemes given above. By writing them both in a more general way, the implicit and explicit schemes are given by

$$\frac{\theta}{\Delta x^2}(u_{i-1,j} - 2u_{i,j} + u_{i+1,j}) + \frac{1-\theta}{\Delta x^2}(u_{i+1,j-1} - 2u_{i,j-1} + u_{i-1,j-1}) = \frac{1}{\Delta t}(u_{i,j} - u_{i,j-1}) \qquad (2.27)$$

where $\theta = 0$ yields the explicit scheme and $\theta = 1$ yields the implicit scheme [4]. However, Crank and Nicolson created a new scheme using $\theta = 1/2$ [4]. This new scheme has a truncation error which goes like $O(\Delta t^2)$ and $O(\Delta x^2)$ which is a great improvement over the previous schemes. Inserting $\theta = 1/2$ into Eq. (2.27) gives

$$\alpha(u_{i-1,j} - 2u_{i,j} + u_{i+1,j} + u_{i+1,j-1} - 2u_{i,j-1} + u_{i-1,j-1}) = 2(u_{i,j} - u_{i,j-1}), \qquad (2.28)$$

and by placing $j-1$ and j terms on either side gives

$$\alpha u_{i-1,j} - \alpha 2u_{i,j} - 2u_{i,j} + \alpha u_{i+1,j} = -\alpha u_{i+1,j-1} + \alpha 2u_{i,j-1} - 2u_{i,j-1} - \alpha u_{i-1,j-1}. \qquad (2.29)$$

By multiplying both sides by -1 and writing this in matrix vector form gives

$$(2\hat{I} + \alpha\hat{B})V_j = (2\hat{I} - \alpha\hat{B})V_{j-1}, \qquad (2.30)$$

where $\hat{I}$ is the identity matrix and $\hat{B}$ is a tri-diagonal matrix

$$\begin{vmatrix} 2 & -1 & 0 & \dots & 0 \\ -1 & 2 & -1 & \dots & 0 \\ 0 & -1 & \dots & \dots & \dots \\ \dots & \dots & \dots & \dots & -1 \\ 0 & 0 & \dots & -1 & 2 \end{vmatrix}$$

It is easy to understand from Eq. (2.30) that the right hand side can be solved using the forward method, and afterwards, using the Thomas algorithm to find V_j.

2.5 Solving the diffusion equation numerically in two dimensions

The method for solving the two-dimensional diffusion equation with the implicit scheme is by using the Jacobi solver, which is an iterative method. The reason for this is that the initial and boundary conditions are not enough to reach a solution for the next time step.

The two dimensional diffusion equation is given by Eq. (2.11). By discretising space with centred difference and discretising time with the backward method gives three equations,

$$u_{xx} \approx \frac{u_{i+1,j}^l - 2u_{i,j}^l + u_{i-1,j}^l}{\Delta x^2}, \qquad (2.31)$$

$$u_{yy} \approx \frac{u_{i,j+1}^l - 2u_{i,j}^l + u_{i,j-1}^l}{\Delta y^2}, \qquad (2.32)$$

$$u_t \approx \frac{u_{i,j}^l - u_{i,j}^{l-1}}{\Delta t}, \qquad (2.33)$$

where now the spacial indices are i and j and the time index is l. The local approximation error of u_{xx} and u_{yy} goes like $O(\Delta x^2)$ and $O(\Delta y^2)$, respectively. The local approximation error to u_t goes like $O(\Delta t)$. When these three are put together this gives the following equation

$$\alpha\left[u_{i+1,j}^l + u_{i-1,j}^l + u_{i,j+1}^l + u_{i,j-1}^l - 4u_{i,j}^l\right] = u_{i,j}^l - u_{i,j}^{l-1} \qquad (2.34)$$

where $\alpha = \Delta t / \Delta x^2$ and we make the assumption that it is a square lattice, i.e $\Delta x = \Delta y$. This equation can be simplified by renaming the following components as $\Delta_l^{i,j}$

$$\Delta_{i,j}^l = u_{i+1,j}^l + u_{i-1,j}^l + u_{i,j+1}^l + u_{i,j-1}^l, \tag{2.35}$$

which leads to

$$u_{i,j}^l = \frac{1}{(1+4\alpha)} \left[\alpha \Delta_{i,j}^l + u_{i,j}^{l-1} \right]. \tag{2.36}$$

Now on the left hand side is an unknown, but on the right hand side are both known variables and unknown variables. Hence, in order to solve this equation it is necessary to use an iterative solver like the Jacobi method which makes an initial guess for the unknown variables on the right hand side. After each iteration this guess becomes better and better. The method for the Jacobi algorithm is given in Algorithm 1. The analytic solution to the two-dimensional equation is given in appendix B.

Algorithm 1: THE JACOBI METHOD: with parallelisation package OpenMP

---

1 N = length of the lattice.
2 MaxIterations = 100,000
3 matrix `Aprev` = solution from previous time step.
4 matrix `Aold` = 1.0 for all i and j

```
/* Start the iterative solver */
```
5 for $k = 0,1,2,\ldots,$ *MaxIterations* do
6   sum = 0.0
7   pragma omp parallel default(shared) private(i,j) reduction(+:sum)
8   pragma omp for
9   for $i = 1,2,\ldots N$-1 do
10   for $j = 1,2,\ldots N$-1 do
11   A(i,j) = (1/(1 + 4*alpha))*(Aprev(i,j) + alpha*(Aold(i+1,j)
12   + Aold(i,j+1) + Aold(i-1,j) + Aold(i,j-1)))

```
        /* Sum the error at each location and make Aold = A for the next iteration.
           */
```
13   for $i = 1,2,\ldots N$-1 do
14   for $j = 1,2,\ldots N$-1 do
15   sum += fabs(Aold(i,j) - A(i,j))
16   Aold(i,j) = A(i,j)

```
        /* End parallel task.  */
```
17

```
        /* Check if the error reach the stopping criteria */
```
18
19   sum = sum/(N*N)
20   if *sum is less than abstol* then
21   return k

```
    /* Jacobi solver reached MaxIterations without convergence */
```
22 return MaxIterations

```
    /* End of function */
```

2.6 Simulating heat diffusion in the Earth's lithosphere in two dimensions

The two dimensional diffusion equation in section 2.5 has the physical constants scaled away in order that the equations are dimensionless. Since in this report we study the temperature diffusion in the lithosphere, we will use physical units for this problem. The equation becomes

$$k \left(\frac{\partial^2 T(x,y,t)}{\partial x^2} + \frac{\partial^2 T(x,y,t)}{\partial y^2} \right) + Q = c_p \rho \frac{\partial T(x,y,t)}{\partial t}, \qquad (2.37)$$

where T is the temperature, ρ is the density, k is the thermal conductivity, c_p is the specific heat capacity and Q is the heat production from radioactive elements. The lithosphere is assumed to have a constant density of $3.510 \, \text{kg/m}^3$, a constant thermal conductivity of $2.5 \, \text{W/m/}^\circ\text{C}$ and a constant specific heat capacity of $1000 \, \text{J/kg/}^\circ\text{C}$. Inside the lithosphere the quantity of radioactive elements varies, and it is separated into three regions. From $0 \, \text{km}$ to $20 \, \text{km}$ in depth (the upper crust) the heat production is $1.40 \, \mu\text{W/m}^3$, from $20 \, \text{km}$ to $40 \, \text{km}$ in depth (the lower crust) the heat production is $0.35 \, \mu\text{W/m}^3$ and between $40 \, \text{km}$ and $120 \, \text{km}$ (the mantle) the heat production is $0.05 \, \mu\text{W/m}^3$.

When radioactive enrichment occurs, the mantle become enriched with uranium, thorium and potassium, which further contribute to the heat production in this region. These elements each have their own half lives. Therefore, to compute the heat production as a function of time the following equation is used:

$$Q(t) = Q(t=0) \left[0.4 \left(\frac{1}{2} \right)^{t/\text{U}_{1/2}} + 0.4 \left(\frac{1}{2} \right)^{t/\text{Th}_{1/2}} + 0.2 \left(\frac{1}{2} \right)^{t/\text{K}_{1/2}} \right], \qquad (2.38)$$

where the heat production 1 Gyr ago, $Q(t=0)$ is assumed to be equal to $0.5 \, \mu\text{W/m}^3$. $\text{U}_{1/2}$ is the half life of uranium equal to $4.47 \, \text{Gyr}$, $\text{Th}_{1/2}$ is the half life of thorium equal to $14.0 \, \text{Gyr}$ and $\text{K}_{1/2}$ is the half life of potassium equal to $1.25 \, \text{Gyr}$. The values 0.4 and 0.2 in front of the half-life equations indicate the elements relative contribution to the heat production. The thermal boundary conditions of the lithosphere are assumed to be 8°C at the top of the upper crust and 1300°C at the bottom of the mantle. Note that all quantities have been scaled in the code script with units in kilograms, joules, gigayears, and kilometres for consistency, although in this report text they may not be. To accommodate the initial conditions and the physical constants, the two-dimensional diffusion equation is altered as shown below:

$$k(u_{xx} + u_{yy}) + Q = c_p \rho u_t. \qquad (2.39)$$

The constant can be moved around giving

$$\frac{k}{c_p \rho}(u_{xx} + u_{yy}) + \frac{Q}{c_p \rho} = u_t, \qquad (2.40)$$

and after discretising this equation in a similar way as done above we get

$$u_{i,j}^l = \frac{1}{1 + 4k\alpha\beta} \left[k\alpha\beta\Delta_{i,j}^l + Q\Delta t\beta + u_{i,j}^{l-1} \right], \qquad (2.41)$$

where $\beta = 1/(c_p\rho)$. Note that the heat production Q can be dependant on both spatial position and time.

3 Method

Our programs are written in C++ and Python. C++ is used to calculate the numerical solutions of the diffusion equation as well as the analytical solution. The C++ linear algebra library Armadillo is used for the handling of vectors and matrices. The results are saved in `.csv` files, and the plotting of the results is done in Python using the Matplotlib library. The C++ program was parallelised using OpenMP in order to speed up the computation time.

3.1 One-dimensional diffusion equation solvers

The one-dimensional diffusion solver was run with spatial step $\Delta x = 0.01$ and timestep $\Delta t \approx 5 \times 10^{-5}$ to compare the numerical solution with the analytical solution. Another experimental run was with parameters $\Delta x = 0.1$ and $\Delta t \approx 6 \times 10^{-3}$. In each of these cases Δt was calculated according to the stability criterion for the explicit case, using $\Delta t = \frac{1}{2}\Delta x^2$. The boundary conditions and initial condition were as specified in Eqs. (2.7, 2.8, 2.9).

3.2 Two-dimensional diffusion equation solver

The two dimensional diffusion solver was run in the dimensionless case to compare the numerical solution with the analytic solution. For the 2D case, only the implicit Jacobi algorithm was implemented and used. The test runs were performed with $\Delta t = 5 \times 10^{-5}$ and $\Delta x = 1 \times 10^{-2}$ as shown in Figs. 4.5 and 4.6. Another set of runs was done with $\Delta t = 1 \times 10^{-3}$ and $\Delta x = 1 \times 10^{-2}$, and also $\Delta t = 1 \times 10^{-2}$ and $\Delta x = 1 \times 10^{-2}$. For the final results for simulating the lithosphere the values $\Delta t = 1 \times 10^{-4}$ and $\Delta x = \Delta y = 1 \times 10^{-2}$ were used. The tolerance used for the Jacobi solver was 1×10^{-5}, which we decided was sufficient when calculating temperatures between 8°C and 1300°C. Prior to this, in the dimensionless case, the tolerance used was 1×10^{-14}. 8°C and 1300°C were the boundary conditions for the top and bottom respectively. The boundary conditions for the vertical sides, at $x = 0$ and $x = 120\,\mathrm{km}$, were both set to 8°C when calculating the final results.

4 Results

4.1 Analytic and Numerical solutions to the one-dimensional diffusion equation

Figs. 4.1 and 4.2 show the solutions of the one-dimensional diffusion equation at two distinct time points for $N_x = 10$ and $N_x = 100$ respectively. The figures show the analytical solution, the numerical solutions using the explicit, implicit and Crank-Nicolson schemes, and the linear, steady-state solution x/L.
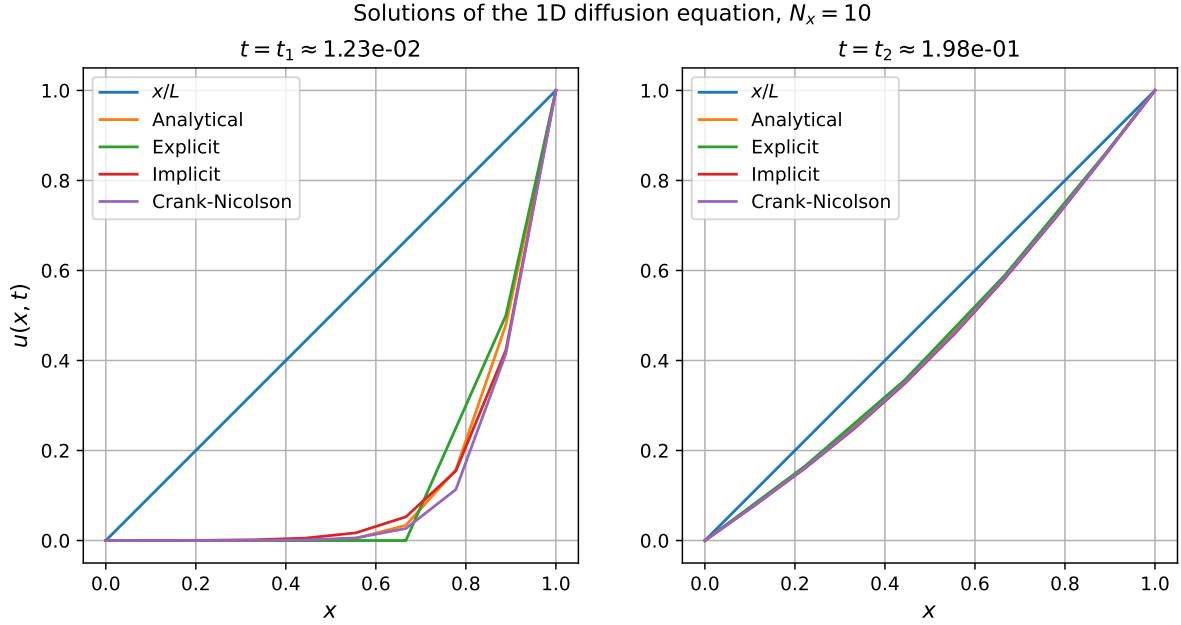

Figure 4.1: The solution to the one dimensional diffusion equation for all schemes with $\Delta x \approx 0.1$ at a time point $t_1 \approx 1.23 \times 10^{-2}$ when $u(x,t)$ is very curved (left plot) and at a time point $t_2 \approx 1.98 \times 10^{-1}$ when $u(x,t)$ is close to linear. The timestep is $\Delta t \approx 6.2 \times 10^{-3}$.

Figs. 4.3 and 4.4 contain colorplots showing the time evolution of the solutions of the one-dimensional diffusion equation for $N_x = 10$ and $N_x = 100$ x values, respectively.
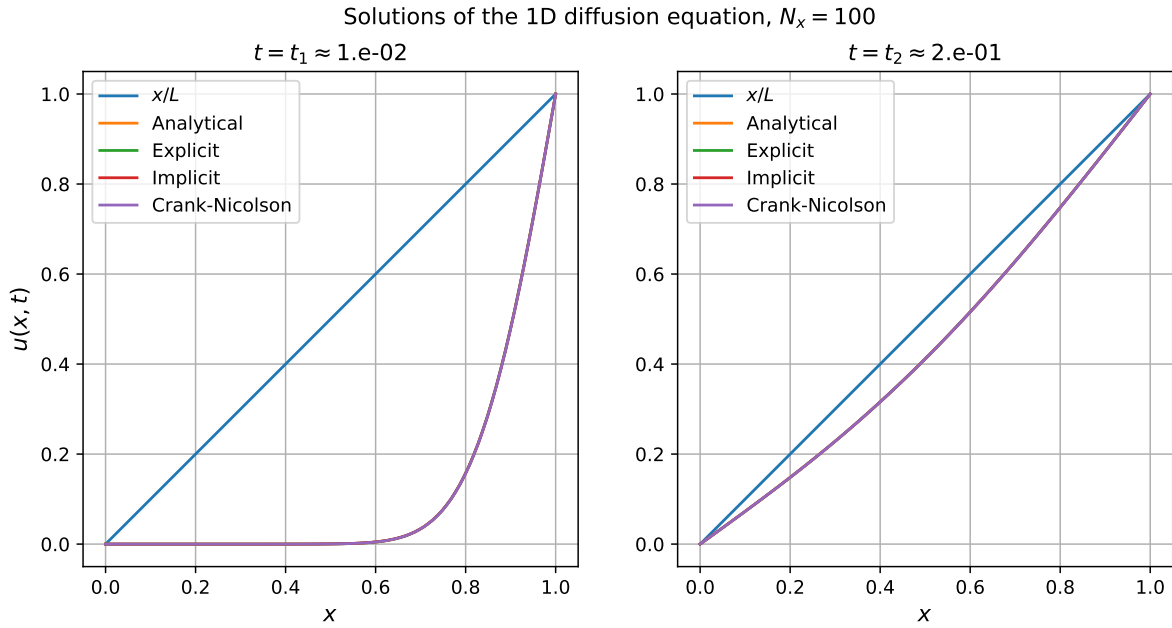
Figure 4.2: The solution to the one dimensional diffusion equation for all schemes with $\Delta x \approx 0.01$ at a time point $t_1 \approx 1.0 \times 10^{-2}$ when $u(x, t)$ is very curved (left plot) and at a time point $t_2 \approx 2.0 \times 10^{-1}$ when $u(x, t)$ is close to linear. The timestep is $\Delta t \approx 5.1 \times 10^{-5}$.
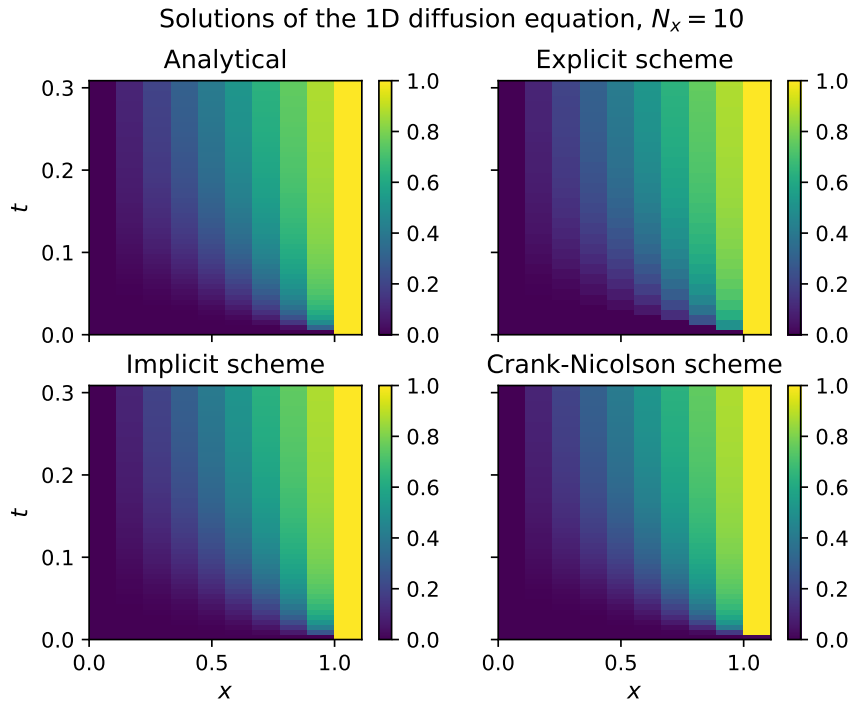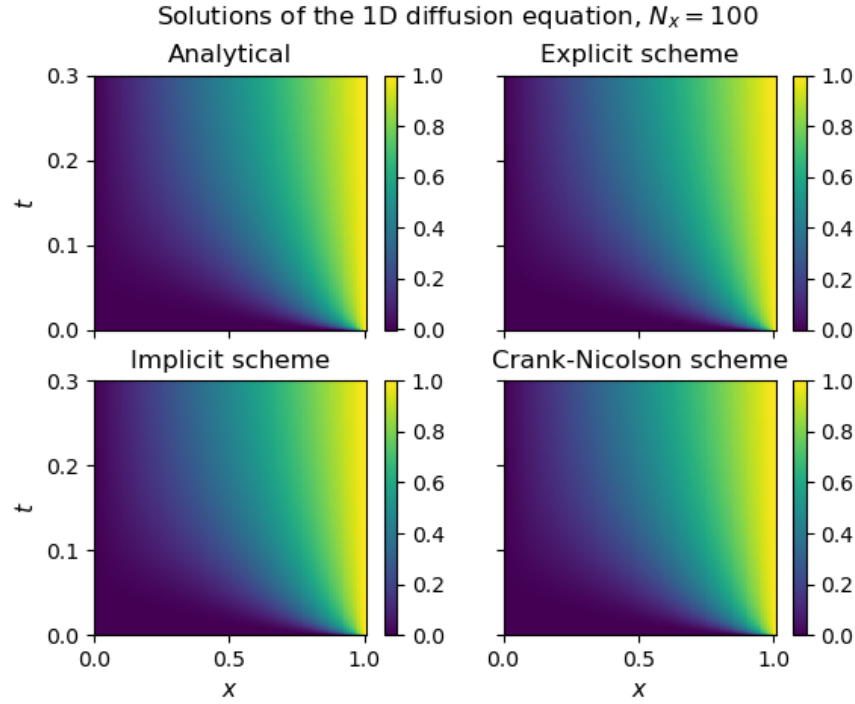
Figure 4.3: Color plots showing the solution of the one dimensional diffusion equation found with four different approaches: the analytical solution, the explicit scheme, the implicit scheme and the Crank-Nicolson scheme. The x axis shows the spatial component x between $x = 0$ and $x = 1$, and the y axis shows the time t. There are $N_x = 10$ evenly spaced points, which gives a step size of $\Delta x = 1/9 \approx 1/10$. The number of terms included in the sum of the analytical solution (see Eq. (2.10)) is $10\,000$. The timestep is $\Delta t = \frac{1}{2}\Delta x^2 \approx 6.17 \cdot 10^{-3}$.

Figure 4.4: Color plots showing the solution of the one dimensional diffusion equation found with four different approaches: the analytical solution, the explicit scheme, the implicit scheme and the Crank-Nicolson scheme. The x axis shows the spatial component x between $x = 0$ and $x = 1$, and the y axis shows the time t. There are $N_x = 100$ evenly spaced points, which gives a step size of $\Delta x = 1/99 \approx 1/100$. The number of terms included in the sum of the analytical solution (see Eq. (2.10)) is 10 000. The timestep is $\Delta t = \frac{1}{2}\Delta x^2 \approx 5.10 \cdot 10^{-5}$.

4.2 Analytic and numerical solutions of the two-dimensional diffusion equation

Figs. 4.5 and 4.6 show the analytical and numerical solutions, respectively, of the two-dimensional diffusion equation. All numerical solutions in the case of two spatial dimensions have been solved using the implicit Jacobi algorithm, which is based on the implicit scheme.
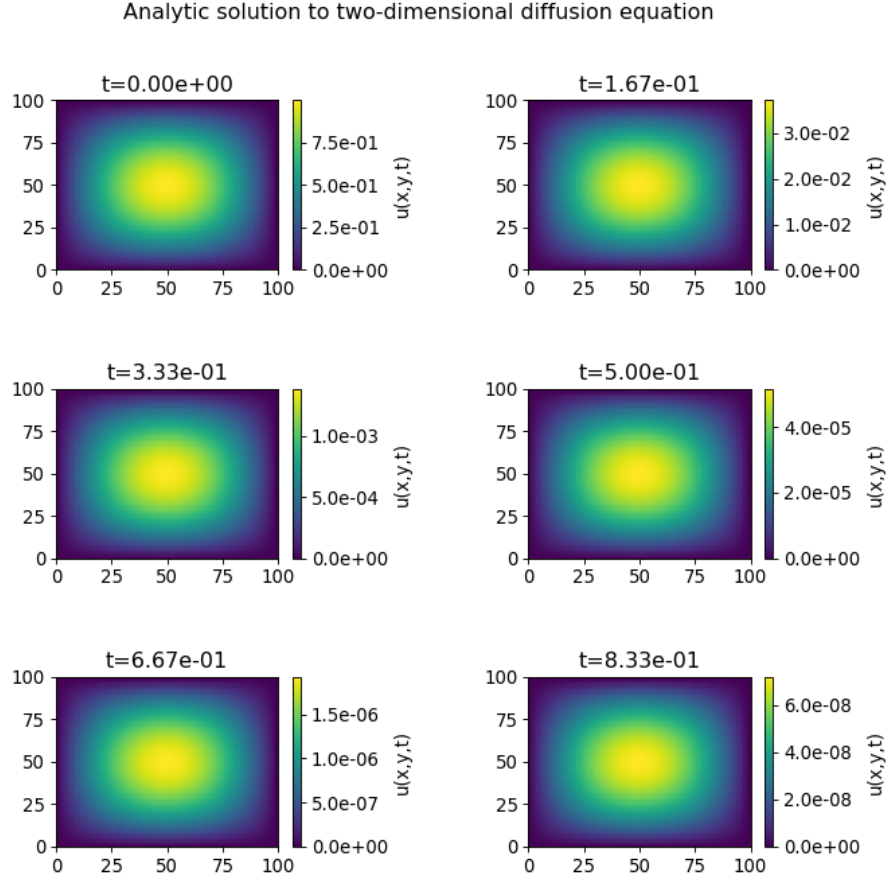

Figure 4.5: Analytic solution to the 2D diffusion equation with $\Delta t = 5 \times 10^{-5}$ and $\Delta x = 0.01$. The x- and y axes show the number of Δx increments; the range is between $x = 0$ and $x = 1$. The code script results a file with 20,000 time points. Six of these time points are shown in the figure. Note that the bars on the side of each subplot shows the scale of the colours in the plot.

A similar comparison is seen in Figs. 4.7 and 4.8, where $u(x, y, t)$ has been plotted as a function of x at a fixed $y = 0.5$ for $\Delta t = 1 \times 10^{-3}$ and $\Delta t = 5 \times 10^{-5}$ respectively.

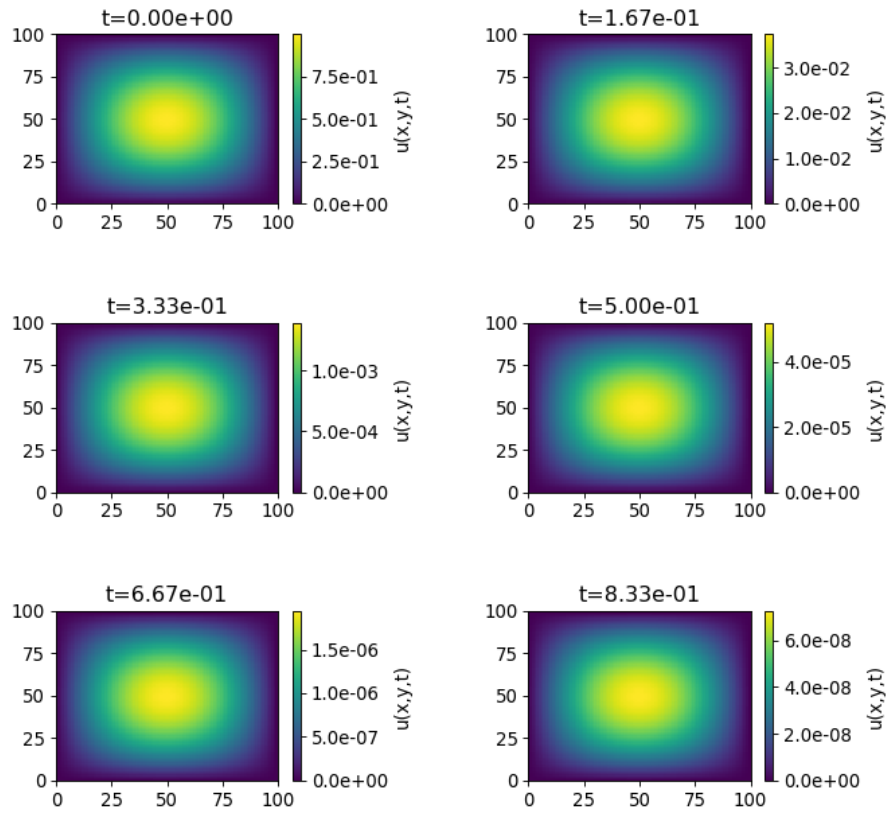Numerical solution to two-dimensional diffusion equation

t=0.00e+00

t=1.67e-01

t=3.33e-01

t=5.00e-01

t=6.67e-01

t=8.33e-01

Figure 4.6: Numerical solution to the 2D diffusion equation with $\Delta t = 5 \times 10^{-5}$ and $\Delta x = 0.01$. The x- and y axes show the number of Δx increments; the range is between $x = 0$ and $x = 1$. The code script results a file with 20,000 time points. Six of these time points are shown in the figure. Note that the bars on the side of each subplot shows the scale of the colours in the plot.
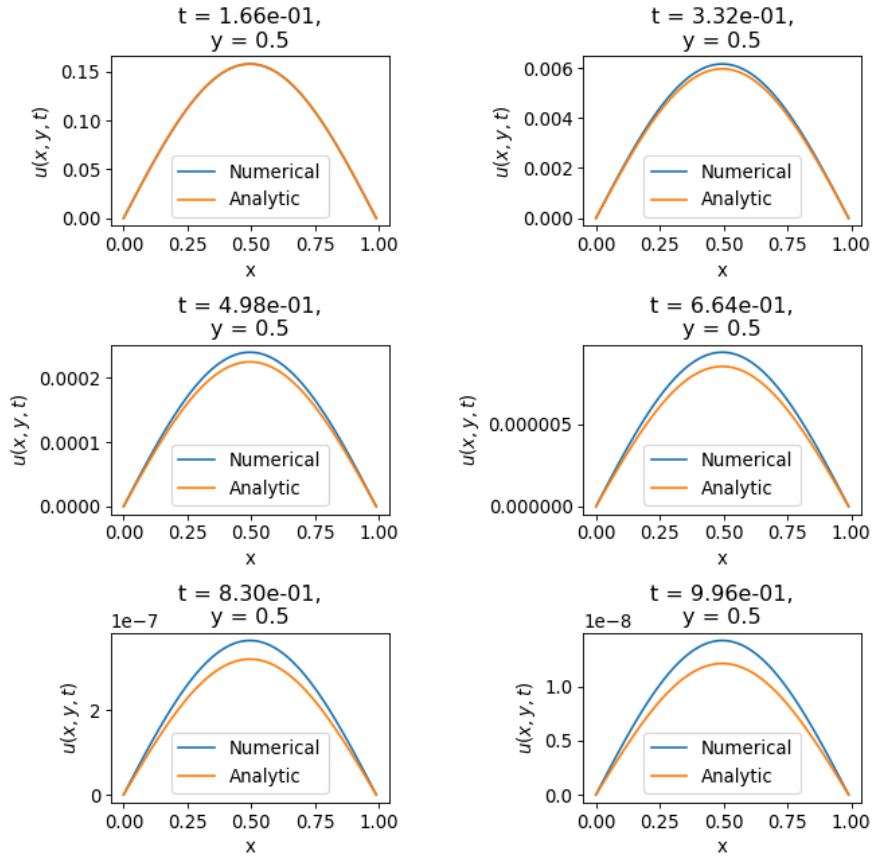
Figure 4.7: Comparison of the numerical and analytic solution to the 2D diffusion equation with $\Delta t = 1 \times 10^{-3}$ and $\Delta x = 0.01$ at a fixed $y = 0.5$.
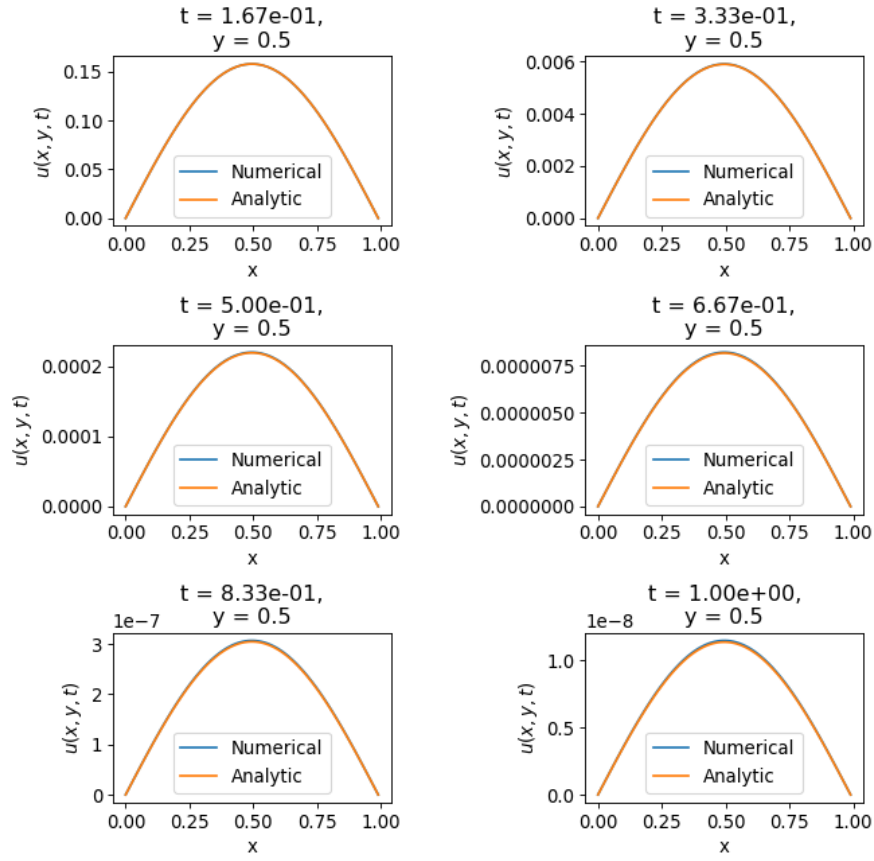
Figure 4.8: Comparison of the numerical and analytic solution to the 2D diffusion equation with $\Delta t = 5 \times 10^{-5}$ and $\Delta x = 0.01$ at a fixed $y = 0.5$.

4.3 Studies of the temperature distribution of the lithosphere

4.3.1 Temperature in the lithosphere without radioactive enrichment

Fig. 4.9 shows the temperature distribution without radioactive enrichment in the mantle. The heat production as a function of depth that does not come from radioactive sources is included. The heat production in the upper crust, lower crust and mantle is $1.4\,\mu\mathrm{W/m^3}$, $0.35\,\mu\mathrm{W/m^3}$ and $0.05\,\mu\mathrm{W/m^3}$, respectively. In Fig. 4.9 the side boundary conditions are $8°\mathrm{C} = 281.15\,\mathrm{K}$, the same as the top surface of the upper crust. It is found that in the first time step (10^5 years) after enrichment the mantle is at maximum $129\,\mathrm{K}$ hotter than before the enrichment. On average, the temperature increases by $131\,\mathrm{K}$ over a period of $1\,\mathrm{Gyr}$.
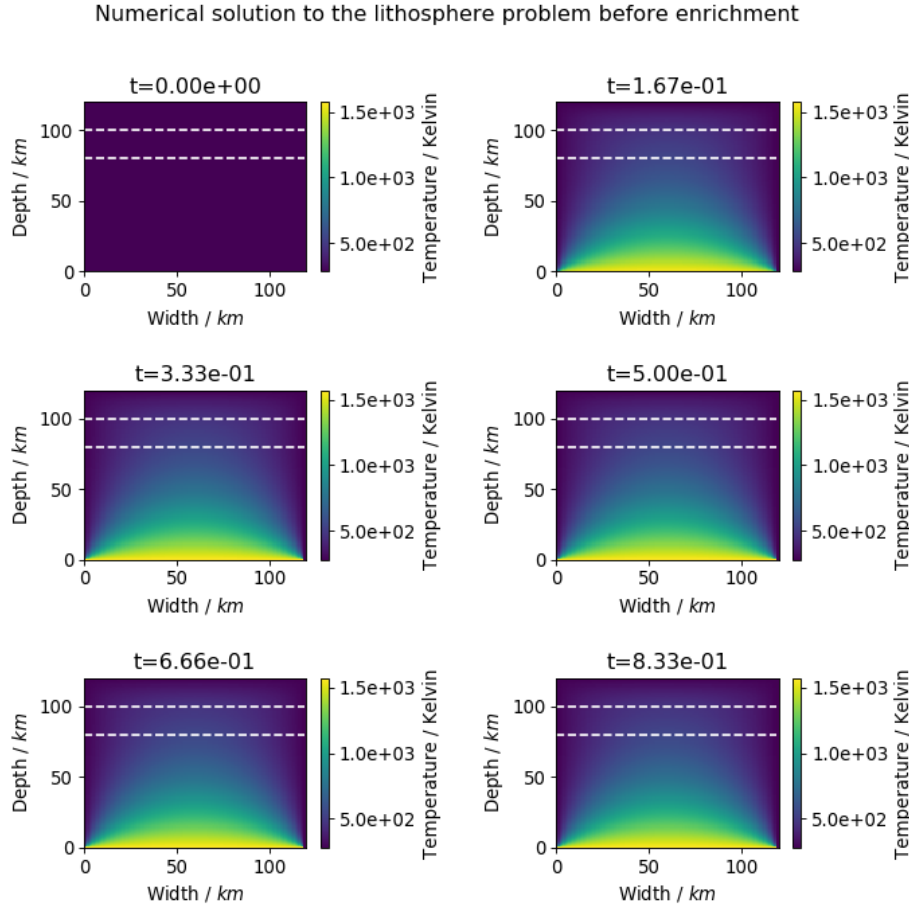

Figure 4.9: Temperature in the lithosphere beginning $1.0\,\mathrm{Gyr}$ ago till the present. The figure shows six time steps in the range between $1.0\,\mathrm{Gyr}$ ago to the present. The x- and y axes of each subplot span $120\,\mathrm{km}$ in width and $120\,\mathrm{km}$ in depth. The boundary conditions are $8°\mathrm{C} = 281.15\,\mathrm{K}$ at the surface and sides, and $1300°\mathrm{C} = 1573.15\,\mathrm{K}$ at the bottom. The white dashed lines indicate the boundary between the upper and lower crust and also between the lower crust and the mantle.

4.3.2 Temperature in the lithosphere with radioactive enrichment

Fig. 4.10 shows the evolution of the lithosphere after being enriched $1\,\mathrm{Gyr}$ ago with uranium, thorium and potassium. The figure does shows some difference to Fig. 4.9 in the temperature distribution, though

this is better visible in Fig. 4.11. Fig. 4.11 shows a cross-section of Figs. 4.9 and 4.10. The cross-section was chosen by taking the middle column, which is the area that is least influenced by the side boundary condition.
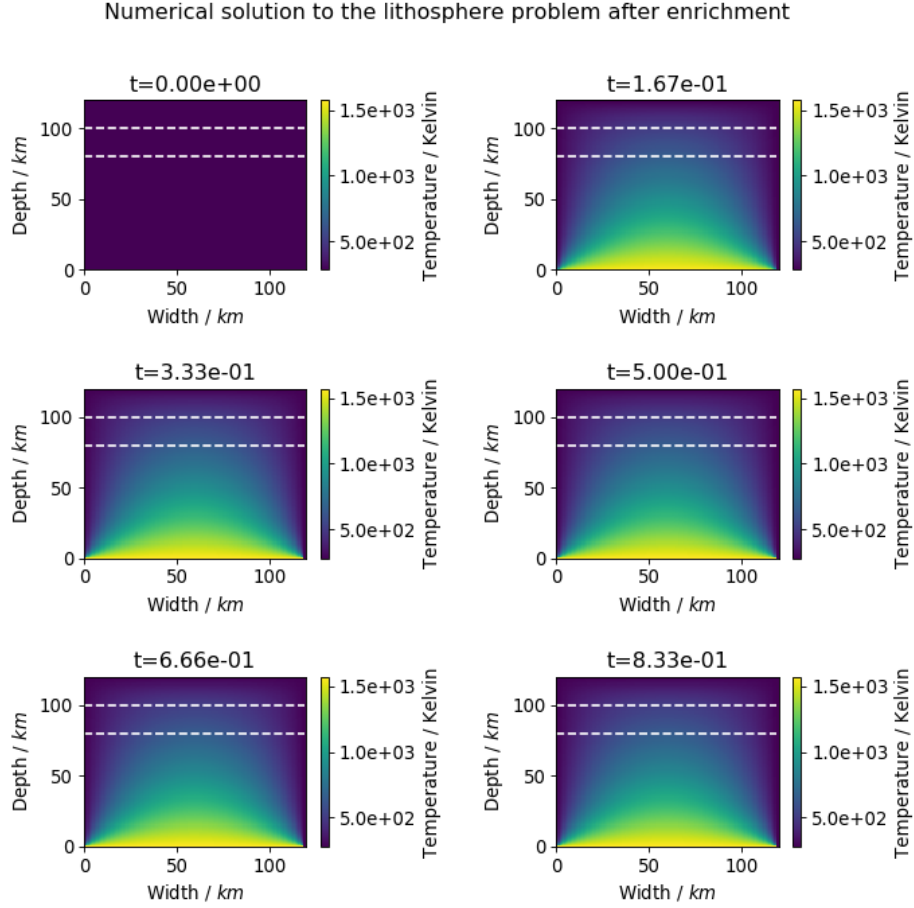

Figure 4.10: Temperature in the lithosphere with radioactive enrichment beginning $1.0\,\mathrm{Gyr}$ ago till the present. The figure shows six time steps in the range between $1.0\,\mathrm{Gyr}$ ago to the present. The x- and y axes of each subplot span $120\,\mathrm{km}$ in width and $120\,\mathrm{km}$ in depth. The boundary conditions are $8°\mathrm{C} = 281.15\,\mathrm{K}$ at the surface and sides, and $1300°\mathrm{C} = 1573.15\,\mathrm{K}$ at the bottom. The white dashed lines indicate the boundary between the upper and lower crust and also between the lower crust and the mantle.

Fig. 4.11 shows that after enrichment the temperature in the upper crust, lower crust and mantle are larger than before enrichment. The maximum difference in temperature between before and one time step (10^5 years) after enrichment is $129\,\mathrm{K}$, which lies in the mantle. After $1\,\mathrm{Gyr}$ the maximum temperature difference between the enriched mantle and normal mantle is calculated to be $292\,\mathrm{K}$. By averaging over depth, the mean temperature difference in the mantle between before and one time step after enrichment is $98\,\mathrm{K}$ with standard deviation $34\,\mathrm{K}$. The figure shows that as time goes on the temperature in the lithosphere increases. Again by averaging over depth, the difference in temperature directly after enrichment and $1\,\mathrm{Gyr}$ later is on average $131\,\mathrm{K}$ with standard deviation of $39\,\mathrm{K}$. This increase in temperature is likely due to the heat production from radioactivity.

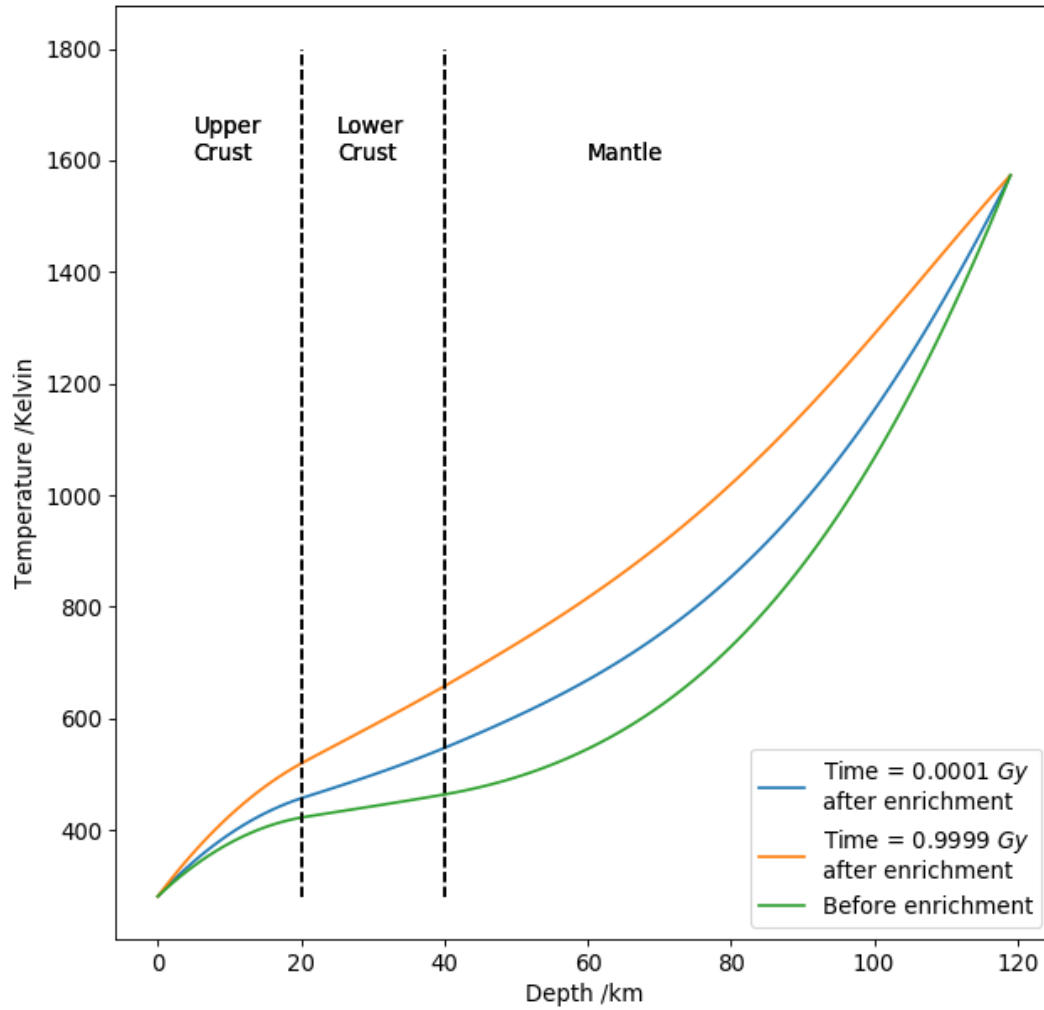A cross-section of the lithosphere comparing temperature distribution before and after radioactive enrichment

Figure 4.11: The temperature distribution in the lithosphere with and without radioactive enrichment in the mantle 1 Gyr ago.

5 Discussion

The comparison between the numerical solutions and the analytical solution seen in Figs. 4.1 and 4.2 indicate that all of the numerical schemes agree either fairly well or very well with the analytical solution. All of the numerical methods are consistent with our initial and boundary conditions, that the temperature should initially be non-zero only at $x = L = 1$ and then diffuse towards the linear steady-state, as in the analytical solution. For the case of $N_x = 100$ points along the x axis, as seen in Fig. 4.2, all of the numerical methods are indistinguishable from the analytical solution. For the case of $N_x = 10$ we are able to see differences between the different schemes, especially for the left graph at $t = t_1$. Here we see that the algorithms based on the implicit and Crank-Nicolson schemes seem to perform better than the explicit algorithm. The implicit method and the Crank-Nicolson method agree better or worse with the analytical solution at different points, so it is not obvious which method of the two is better by looking at this graph.

The time evolutions of the solutions of the one-dimensional case, seen in the colorplots in Figs. 4.3 and 4.4, are as expected. At $t = 0$ most of the solvers have the initial conditions of $u(x, t = 0) = 0$ everywhere except for at $x = L$ where it is $u(x = L, t = 0) = 1$. For an unknown reason, the Crank-Nicolson algorithm is initially (approximately) zero everywhere at $t = 0$, including at $x = L$, in the case of $N_x = 10$. But at $t > 0$ it gave the correct value of $u(x = L, t) = 1$, so it seems that the solver works good for all other time points. This could be caused by an error in our code or a bug caused by some feature in the Crank-Nicolson scheme that we are unaware of. In the $N_x = 100$ case this is not an apparent problem. Using the interpretation of $u(x, t)$ as the temperature in space and time, the solutions start in a state where the temperature is high only in one place at $x = L$, and in time the temperature diffuses toward the colder side at $x = 0$ until the system reaches its equilibrium temperature distribution. By looking at these colorplots, the time to reach equilibrium is seen to be around $t = 0.2$ or slightly less. The results are seen in higher resolution in the $N_x = 100$ case (Fig. 4.4), both temporally and spatially, compared to the $N_x = 10$ case (Fig. 4.3).

For the two-dimensional diffusion equation, when comparing the analytical solution (Fig. 4.5) and the numerical solution (Fig. 4.6) we see a very good agreement between them. The six subplots in each of the figures look pretty much identical, but each of the six subplots have a different colour scale, indicated by the bars at the side of each subplot. The boundary conditions are that all four walls have zero temperature for all t. Sticking with the temperature interpretation of the diffusion equation, the four walls act like heat sinks in the system. Initially all of the thermal energy is contained inside the two-dimensional area, and the temperature inside the area is maximal at this initial time. Over time, the temperature diffuses from the hotter interior to the colder walls since the thermal energy is transferred to the colder walls in order to reach thermal equilibrium. Since there are no heat sources in this case and only an initial temperature distribution, we should expect the steady state of the system to be zero temperature everywhere, that is, $u(x, y, t \to \infty) = 0$ for all positions (x, y). This is consistent with the analytical expression seen in Eq. (2.14), which has an inverse-exponential factor in time. This is what we observe in the colorplot figures as well; the colorbars indicate that the maximum temperature is decreasing for each timestep.

In Figs. 4.7 and 4.8 the effect of Δt on the accuracy of the solver becomes apparent. The smaller time interval of $\Delta t = 5 \times 10^{-5}$ (Fig. 4.8) agrees better with the analytic solution compared to $\Delta t = 1 \times 10^{-3}$ (Fig. 4.7).

The results in Fig. 4.9 show that the boundary conditions on the sides of the lithosphere are important. Different boundary conditions were tested, and the results show that they change the temperature distribution depending on their value. While the cross-section of the crust is seen as a 2D cross-section, the temperature distribution at each depth is equal everywhere at that depth in this problem. So the problem can actually be reduced to one dimension. In fact, it would be more accurate to do it in one dimension, because in the 2D case the algorithm requires boundary conditions at each of the four sides of the 2D area we are solving the diffusion equation for. The top side (the surface) and the bottom side (the bottom of the lithosphere) have well defined boundary conditions for the temperature, but using

such simple boundary conditions for the vertical sides is not realistic since we expect the temperature to increase steadily with depth. The most accurate boundary conditions for the vertical sides would actually be the solution of the 1D problem using the top and bottom temperatures as the boundary conditions, so the 2D solver is not necessary for this specific problem. This is also discussed in the Outlook section.

The lithosphere results also show that the radioactive enrichment has a non-negligible effect on the temperature distribution in the lithosphere. In time, the heat production of the enriched mantle decreases because of radioactive decay, but the temperature is still increasing. The boundary conditions on the vertical sides, at $x = 0$ and $x = 120$ km, were found to have an big influence on the time development of the temperature distribution. On the other hand, the same boundary conditions were used before and after enrichment. This means that the *relative* temperature difference between the two cases should be quite realistic. In addition to this, the curves in Fig. 4.11 are taken from the middle of the lithosphere, at $x = 60$ km, in Figs. 4.9 and 4.10. This minimises the effects of the boundary conditions at the vertical sides.

6 Conclusion

By comparing the numerical solutions of the one-dimensional diffusion equation with the analytical solution, we have found that the implicit scheme and the Crank-Nicolson scheme outperforms the explicit scheme with regard to accuracy. Either one of these two methods seem to be a good choice for solving the diffusion equation with good accuracy.

In the two-dimensional case it was found that the implicit scheme solved using Jacobi's iterative method agreed well with the analytic solution. The length of the timestep Δt was seen to affect the accuracy of the numerical solver, so a sufficiently low timestep should be used. We found that $\Delta t = 5 \times 10^{-5}$ gave good agreement with the analytical solution in the case of $\Delta x = \Delta y \approx 0.01$.

These algorithms were applied to studying the evolution of the lithosphere based on the theory that a subducting zone on the western coast of Norway caused radioactive enrichment in the mantle $1\,\mathrm{Gyr}$ ago. The simulations implemented here suggest that the temperature in the mantle $1\,\mathrm{Gyr}$ ago would be at maximum $129\,\mathrm{K}$ greater than before enrichment. At the present, the temperature in the mantle if found to be at maximum $292\,\mathrm{K}$ greater than if it had not been enriched $1\,\mathrm{Gyr}$ ago.

7 Outlook

The 2D variants of the numerical solutions of solving the diffusion equation are useful and necessary for simulating systems or solve problems that cannot be reduced to one dimension. However, as mentioned in the Discussion section, our lithosphere problem was in fact essentially a one-dimensional problem, and using the one-dimensional solution or solvers would actually be better suited and give the most accurate results. Also, the computation time would decrease. So we would advise to use the one-dimensional solvers or the analytical solution for this specific problem.

Another point regarding the 2D case: it would have been useful to have an analytical 2D solution to be able to compare the results for the lithosphere temperature with. This could have been achieved by using different boundary- and initial conditions than we used in our derivation of the 2D solution. The 1D analytical solution, as seen in Eq. (2.10), is only valid for the specific boundary conditions of $u(x = 0, t) = 0$ and $u(x = L, t) = 1$. If we wanted to study a problem with different boundary conditions, we would have to derive the solution again with different boundary- and initial conditions. This is also the case for the 2D solution. The boundary conditions we used were $u(x, y, t) = 0$ at all four sides $(x = 0, L$ and $y = 0, L)$, and the initial condition we used was a product of two sinusoidal functions. See appendix B for more details. This initial condition was chosen since it was then trivial to get the Fourier coefficients required to find the analytical solution. By using the proper boundary- and initial conditions in the derivation, an analytical solution equivalent to the numerical solutions could have been found, and the two could have been compared. The reason why we didn't do the derivation again for these initial conditions was because of time constraints. However, this comparison can definitely be useful for any people studying this problem in the future in order to test the accuracies of the 2D solvers.

8 Github address

Github address: `https://github.com/amundwf/comp-phys-project5.git`

References

[1] Morten Hjorth Jensen. Computational physics, diffusion equation, 2020. `https://github.com/CompPhysics/ComputationalPhysics/blob/master/doc/Projects/2020/Project5/DiffusionEquation/pdf/DiffusionEquation.pdf`, Retrieved December 14, 2020.

[2] Jianping Zheng, Qing Xiong, Yi Zhao, and Wenbo Li. Subduction-zone peridotites and their records of crust-mantle interaction. *Science China Earth Sciences*, pages 1–20, 2019.

[3] Fabien Deschamps, Marguerite Godard, Stéphane Guillot, and Kéiko Hattori. Geochemistry of subduction zone serpentinites: A review. *Lithos*, 178:96–127, 2013.

[4] Aslak Tveito and Ragnar Winther. *Introduction to partial differential equations: a computational approach*, volume 29. Springer Science & Business Media, 2004.

A Derivation of the analytical solution of the one-dimensional diffusion equation

Here, a detailed derivation of the analytical solution of the one-dimensional diffusion equation will be presented. As presented earlier, the diffusion equation is given by

$$\frac{\partial^2 u(x,t)}{\partial x^2} = \frac{\partial u(x,t)}{\partial t} \quad \Longleftrightarrow \quad \frac{\partial^2 u(x,t)}{\partial x^2} - \frac{\partial u(x,t)}{\partial t} = 0. \tag{A.1}$$

The domain in this problem is $0 \leq x \leq L$ and $t \geq 0$.

The boundary conditions of this problem are given by

$$u(0,t) = 0, \quad t \geq 0, \tag{A.2}$$

and

$$u(L,t) = 1, \quad t \geq 0, \tag{A.3}$$

and the initial condition is given by

$$u(x,0) = 0, \quad 0 < x < L. \tag{A.4}$$

To make it easier to calculate the solution, we want to modify $u(x,t)$ to a new function $v(x,t)$ which is zero at both boundaries, that is,

$$v(0,t) = v(L,t) = 0. \tag{A.5}$$

This can be achieved by defining v as

$$v(x,t) \equiv u(x,t) + f(x), \tag{A.6}$$

where $f(x)$ is an unknown function that only varies in space and not in time and makes $v(x,t)$ satisfy the boundary conditions in Eq. (A.5). The end point values of $f(x)$ can then be found:

$$v(0,t) = 0 = u(0,t) + f(0) = 0 + f(0)$$
$$\Updownarrow$$
$$f(0) = 0$$

and

$$v(L,t) = 0 = u(L,t) + f(L) = 1 + f(L)$$
$$\updownarrow$$
$$f(L) = -1.$$

The initial condition for $v(x,t)$ is

$$v(x,0) = u(x,0) + f(x) = 0 + f(x) = f(x). \tag{A.7}$$

We will also assume that $v(x,t)$ is a solution of the diffusion equation, and we will now use this to find the expression for $f(x)$.

$$\partial_{xx}^2 v(x,t) = \partial_t v(x,t) \tag{A.8}$$
$$\partial_{xx}^2 (u(x,t) + f(x)) = \partial_t (u(x,t) + f(x)) \tag{A.9}$$
$$\partial_{xx}^2 u + \partial_{xx}^2 f(x) = \partial_t u + 0 \tag{A.10}$$
$$(\partial_{xx}^2 u - \partial_t u) + \partial_{xx}^2 f(x) = 0 \tag{A.11}$$
$$\partial_{xx}^2 f(x) = 0. \tag{A.12}$$

Eq. (A.12) is an ordinary differential equation that is easily solved by integrating twice:

$$f(x) = \iint \partial^2 f(x)\, dx\, dx$$
$$= \int \left(\int 0\, dx \right) dx$$
$$= \int C\, dx$$
$$= Cx + D$$

for some undetermined constants C and D. These constants are found by using the boundary conditions:

$$f(0) = 0 = C \cdot 0 + D = D$$
$$\updownarrow$$
$$D = 0$$
$$\updownarrow$$
$$f(x) = Cx,$$

and

$$f(L) = -1 = C \cdot L$$
$$\updownarrow$$
$$C = -\frac{1}{L}$$

so we get

$$f(x) = \left(-\frac{1}{L} \right) x = -\frac{x}{L}. \tag{A.13}$$

26

In order to find the solution to the diffusion equation, we will use separation of variables. That is, we will assume that v is of the form $v(x,t) = X(x) \cdot T(t)$. Using this assumption, the diffusion equation becomes

$$\partial_{xx}^2(X(x)T(t)) = \partial_t(X(x)T(t))$$
$$T(t)\partial_{xx}^2 X(x) = X(x)\partial_t T(t)$$
$$\Updownarrow$$
$$\frac{X''(x)}{X(x)} = \frac{T'(t)}{T(t)}.$$

Since the left hand side only depends on x it is constant in t, and since the right hand side only depends on t it is constant in x. Therefore the above equation has to be constant in both t and x, and we can denote this constant as $-\lambda^2$:

$$\frac{X''(x)}{X(x)} = \frac{T'(t)}{T(t)} \equiv -\lambda^2 = \text{constant}. \tag{A.14}$$

Then we have the following equations:

$$X''(x) = -\lambda^2 X(x) \tag{A.15}$$

and

$$T'(t) = -\lambda^2 T(t). \tag{A.16}$$

Eq. (A.15) is an ordinary differential equation with the general solution

$$X(x) = A\sin(\lambda x) + B\cos(\lambda x), \tag{A.17}$$

and Eq. (A.16) has the general solution

$$T(t) = Ce^{-\lambda^2 t}. \tag{A.18}$$

The solution of $v(x,t)$ will therefore have the form

$$v(x,t) = X(x)T(t) = (A\sin(\lambda x) + B\cos(\lambda x)) \cdot Ce^{-\lambda^2 t}. \tag{A.19}$$

The boundary conditions give:

$$v(0,t) = X(0)T(t) = 0$$
$$\downarrow$$
$$X(0) = 0$$
$$(A \cdot 0 + B \cdot 1) = 0$$
$$B = 0$$
$$\Downarrow$$
$$X(x) = A\sin(\lambda x)$$

and

$$v(L,t) = X(L)T(t) = 0$$
$$\downarrow$$
$$X(L) = 0$$
$$A\sin(\lambda L) = 0$$
$$\Updownarrow$$
$$\lambda L = n\pi$$
$$\Downarrow$$
$$\lambda \equiv \lambda_n = \frac{n\pi}{L}$$
$$\Downarrow$$
$$X(x) = A\sin(n\pi x/L) \equiv A_n\sin(\lambda_n x).$$

where $n = 1, 2, \ldots$ and we have chosen $X(0), X(L) = 0$ instead of the trivial solutions $T(t) = 0$. Then the solution of $v(x,t)$ is

$$v(x,t) = A_n\sin(\lambda_n x)\cdot Ce^{-\lambda_n^2 t} \equiv C_n\sin(\lambda_n x)e^{-\lambda_n^2 t} \tag{A.20}$$

Since the diffusion equation linear, any sum of solutions is also a solution to the diffusion equation. So the general solution is the sum of all the possible solutions, which would be a sum over all values of n:

$$v(x,t) = \sum_{n=1}^{\infty} C_n\sin(\lambda_n x)e^{-\lambda_n^2 t}. \tag{A.21}$$

The initial condition gives

$$v(x,0) = f(x) = \sum_{n=1}^{\infty} C_n\sin(n\pi x/L)\cdot 1, \tag{A.22}$$

which is a Fourier series. From the theory of Fourier series, the coefficients are found from the formula

$$C_n = \frac{2}{L}\int_0^L f(x)\sin(n\pi x/L)\,dx. \tag{A.23}$$

With $f(x) = -x/L$ this becomes

$$C_n = \frac{2}{L}\int_0^L \left(-\frac{x}{L}\right)\sin\left(\frac{n\pi}{L}x\right)\,dx$$
$$= -\frac{2}{L^2}\int_0^L x\sin\left(\frac{n\pi}{L}x\right)\,dx$$
$$= -\frac{2}{L^2}\cdot\frac{L^2}{n^2\pi^2}\left(\sin(n\pi) - n\pi\cos(n\pi)\right)$$
$$= -\frac{2}{n^2\pi^2}(0 - n\pi(-1)^n)$$
$$= \frac{2}{n\pi}(-1)^n.$$

where the integral has been looked up. Substituting this expression for C_n into Eq. (A.21) we get the general solution for v,

$$v(x,t) = \frac{2}{\pi}\sum_{n=1}^{\infty}(-1)^n\frac{\sin(n\pi x/L)}{n}e^{-n^2\pi^2 t/L^2}. \tag{A.24}$$

Then finally we find the general solution for $u(x, t)$ from Eq. (A.6):

$$u(x,t) = v(x,t) - f(x) + = \frac{2}{\pi} \sum_{n=1}^{\infty} (-1)^n \frac{\sin(n\pi x/L)}{n} e^{-n^2\pi^2 t/L^2} + \frac{x}{L}. \tag{A.25}$$

B Derivation of the analytical solution of the two-dimensional diffusion equation

Here, a detailed derivation of the two-dimensional diffusion equation is presented. As with the one-dimensional case, again, we assume the separation of variables, i.e,

$$u(x, y, t) = X(x)Y(y)T(t). \tag{B.1}$$

Inserting this into the two-dimensional diffusion equation as presented earlier, the diffusion equation becomes,

$$Y(y)T(t)X_{xx} + X(x)T(t)Y_{yy} = X(x)Y(y)T_t \tag{B.2}$$

$$\frac{X_{xx}}{X} + \frac{Y_{yy}}{Y} = \frac{T_t}{T} \tag{B.3}$$

This can be equated to a constant giving the following equations

$$\frac{X_{xx}}{X} + \frac{Y_{yy}}{Y} = -\nu^2 \tag{B.4}$$

and

$$\frac{T_t}{T} = -\nu^2, \tag{B.5}$$

where ν is a constant. Eq. B.4 can further be re-aranged by introducing another constant κ so that each spatial component is separate. This is shown by the following

$$\frac{X_{xx}}{X} = -\frac{Y_{yy}}{Y} - \nu^2 = -\kappa^2, \tag{B.6}$$

which leads to two equations

$$X_{xx} + \kappa^2 X = 0 \tag{B.7}$$

and

$$Y_{yy} + \rho^2 Y = 0, \tag{B.8}$$

where $\rho^2 = \nu^2 - \kappa^2$. This gives two general equations for the solution of X and Y.

$$X(x) = A\cos\kappa x + B\sin\kappa x \tag{B.9}$$

and

$$Y(y) = C\cos\rho y + D\sin\rho y. \tag{B.10}$$

By assuming boundary conditions of $X(0) = X(L) = Y(0) = Y(L) = 0$ places restrictions on the two equations above. Applying the boundary conditions leads to

$$
\begin{aligned}
X(0) &= A & \longrightarrow & \quad A = 0 \\
Y(0) &= C & \longrightarrow & \quad C = 0 \\
X(L) &= B \sin \kappa L & \longrightarrow & \quad \kappa = n\pi/L \\
Y(L) &= D \sin \rho L & \longrightarrow & \quad \rho = m\pi/L
\end{aligned}
$$

where n and m are equal to $\pm 1, \pm 2, \pm 3...$. The general solution to the temporal component $T(t)$ is the same as in the one dimensional case, $T(t) = \text{Constant} \cdot \exp\left(-\nu^2 t\right)$. This leads to an equation with an infinite sum

$$
u(x, y, t) = \sum_{n=1}^{\infty} \sum_{m=1}^{\infty} A_{nm} \sin\left(\frac{n\pi x}{L}\right) \sin\left(\frac{m\pi y}{L}\right) e^{\frac{-(n^2 + m^2)\pi^2 t}{L^2}}. \tag{B.11}
$$

If we introduce the initial conditions that $u(x, y, 0) = \sin\left(\pi x/L\right)\sin\left(\pi y/L\right)$, this gives

$$
u(x, y, 0) = \sin\left(\frac{\pi x}{L}\right) \sin\left(\frac{\pi y}{L}\right) = \sum_{n=1}^{\infty} \sum_{m=1}^{\infty} A_{nm} \sin\left(\frac{n\pi x}{L}\right) \sin\left(\frac{m\pi y}{L}\right) \tag{B.12}
$$

By using the theory of Fourier series, these coefficients A_{nm} are

$$
A_{nm} = \left(\frac{2}{L}\right)^2 \int_0^L \int_0^L \sin\left(\frac{\pi x}{L}\right) \sin\left(\frac{\pi y}{L}\right) \sin\left(\frac{n\pi x}{L}\right) \sin\left(\frac{m\pi y}{L}\right) dx dy. \tag{B.13}
$$

Using the definition of orthogonal polynomials

$$
\int_0^L \sin\left(\frac{n\pi x}{L}\right) \sin\left(\frac{m\pi x}{L}\right) dx = \begin{cases} \frac{L}{2} & \text{if } n = m \\ 0 & \text{if } n \neq m \end{cases} \tag{B.14}
$$

results in the solution to A_{nm} only when $n = m = 1$,

$$
A_{nm} = \left(\frac{2}{L}\right)^2 \left(\frac{L}{2}\right)^2 = 1. \tag{B.15}
$$

This gives the analytic solution to be

$$
u(x, y, t) = \sin\left(\frac{\pi x}{L}\right) \sin\left(\frac{\pi y}{L}\right) e^{-2\pi^2 t/L^2}, \tag{B.16}
$$

with the specific boundary and initial conditions given above.